PLOS ONE

RESEARCH ARTICLE

Inclusion of hybrid nanoparticles in hyperbolic tangent material to explore thermal transportation via finite element approach engaging Cattaneo-Christov heat flux

Umar Nazir[1], Muhammad Sohail[1]*, Hussam Alrabaiah[2,3], Mahmoud M. Selim[4,5], Phatiphat Thounthong[6], Choonkil Park[7]*

1 Department of Applied Mathematics and Statistics, Institute of Space Technology, Islamabad, Pakistan, **2** College of Engineering, Al Ain University, Al Ain, United Arab Emirates, **3** Department of Mathematics, Tafila Technical University, Tafila, Jordan, **4** Department of Mathematics, Al-Aflaj College of Science and Humanities Studies, Prince Sattam Bin Abdulaziz University, Al-Aflaj, Saudi Arabia, **5** Department of Mathematics, Suez Faculty of Science, Suez University, Suez, Egypt, **6** Research Institute for Natural Sciences, Hanyang University, Seoul, Korea, **7** Renewable Energy Research Centre, Department of Teacher Training in Electrical Engineering, Faculty of Technical Education, King Mongkut's University of Technology North Bangkok, Bangkok, Thailand

* muhammad_sohail111@yahoo.com (MS); baak@hanyang.ac.kr (CP)

Citation: Nazir U, Sohail M, Alrabaiah H, Selim MM, Thounthong P, Park C (2021) Inclusion of hybrid nanoparticles in hyperbolic tangent material to explore thermal transportation via finite element approach engaging Cattaneo-Christov heat flux. PLoS ONE 16(8): e0256302. https://doi.org/10.1371/journal.pone.0256302

Editor: Naramgari Sandeep, Central University of Karnataka, INDIA

Received: June 24, 2021

Accepted: August 3, 2021

Published: August 25, 2021

Data Availability Statement: The data used to support this study are included in the Manuscript.

Funding: This work is supported by the Basic Science Research Program through the National Research Foundation of Korea funded by the Ministry of Education, Science and Technology (NRF-2017R1D1A1B04032937).

Competing interests: The authors have declared that no competing interests exist.

Abstract

This report is prepared to examine the heat transport in stagnation point mixed convective hyperbolic tangent material flow past over a linear heated stretching sheet in the presence of magnetic dipole. Phenomenon of thermal transmission plays a vital role in several industrial manufacturing processes. Heat generation is along with thermal relaxation due to Cattaneo-Christov flux is engaged while modeling the energy equation. In order to improve the thermal performance, inclusion of hybrid nanoparticles is mixed in hyperbolic tangent liquid. The conservation laws are modeled in Cartesian coordinate system and simplified via boundary layer approximation. The modeled partial differential equations (PDEs) system are converted into ordinary differential equations (ODEs) system by engaging the scaling group transformation. The converted system of modeled equations has been tackled via finite element procedure (FEP). The efficiency of used scheme has been presented by establishing the grid independent survey. Moreover, accurateness of results is shown with the help of comparative study. It is worth mentioning that the inclusion of hybrid nanoparticles has significant higher impact on heat conduction as compared with nanoparticle. Moreover, hybrid nanoparticles are more efficient to conduct maximum production of heat energy as compared with the production of heat energy of nanoparticles. Hence, hybrid nanoparticles (MoS_2/Ag) are observed more significant to conduct more heat energy rather than nanoparticle (Ag).

1. Introduction

Non-Newtonian fluids have diverse applications and usage in several engineering disciplines. There constitutive relation is different than Newtonian materials. For non-Newtonian materials, the stress strain relationship is complicated. These materials occur frequently in different phenomenon and it has applications in polymers extrusion, medical, oil-pipeline friction reduction and several others. An important non-Newtonian model is hyperbolic tangent [1–5], whose constitutive expression is expressed as

$$S^* = -PI + \tau^*_{TH}, \tau^*_{TH} = -\dot{\alpha}[\mu_\infty + (\mu_\infty + \mu_0)\tanh(\Gamma^1\dot{\alpha})^m],$$

for $\mu_\infty = 0, \Gamma^1\dot{\alpha} < 1$, we get

$$\tau^*_{TH} = -\dot{\alpha}\mu_0[1 + m(\dot{\alpha} - 1)].$$

Naseer et al. [1] examined the exponentially stretched flow of mixed convective hyperbolic tangent model in horizontal cylinder with thermal transportation. They engaged shooting approach to solve transformed nonlinear boundary layer equations (BLEs). They have discussed the contribution of several influential variables on velocity and temperature. They observed the depreciation in temperature field for higher values of Reynolds number and Prandtl number. Khan et al. [2] used BVPh2.0 package to handle the solution for chemically reactive hyperbolic tangent model undergoing radiation and heat generation phenomenon. They have found that velocity is a diminishing function of Weissenberg number and temperature profile grows against radiation parameter. Nawaz et al. [3] explored the contribution of hybrid nanoparticles in hyperbolic tangent model in a stretched cylinder using finite element approach. They modeled the thermal phenomenon under radiation effect and heat generation. They observed that heat transfer rate of hybrid nanoparticles is higher than nanofluid and it is recommended for better thermal performance. Mathematical analysis for inclined MHD hyperbolic tangent model was studied by Ali et al. [4] via BVP4C package. They recorded the increase in Nusselt number for Prandtl number. Patil and Raju. [5] used the convective conditions in hyperbolic tangent model past over a nonlinear exponential porous stretching sheet. They modeled the energy transport in the presence of viscous dissipation and radiation effect. They used shooting approach to compute solution for the arising boundary layer equations. They concluded that higher values of Eckert number reduce the skin friction and enhances the Sherwood number.

Nanofluids are a hot topic of research due to their wider use in different industrial mechanisms. It is used in several engineering systems to control/enhance the thermal performance. The inclusion of nanoparticles in base fluids enhances the thermal conductivity which enhance in thermal process. Several researchers have a look on this hot topic due to their wider applications and usage. For instance, Aman et al. [6] studied the thermal performance of unsteady convective Casson model by mixing SWCNTs and MWCNTs in a vertical channel. They used the thermal conductivity model which was proposed by Maxwell. They have considered radiation effect in thermal profile and mixed convection along with MHD effect is taken in momentum transport. They presented the perturbation solution for the arising problem. Several graphs and tables are presented by them to notice the influence of emerging parameters on obtained solution. They reported the increase in thermal field by enhancing the values of radiation parameter and volume fraction because it upsurges the conduction. Moreover, they recorded the enhancement in velocity against Richardson parameter. Mixed convective stratified unsteady electrically conducting viscous nanofluid was investigated by Daniel et al. [7]. They modeled a strong problem over a melting stretching sheet with several important physical effects. They modeled a strong problem by taking several important effects like mixed

convection, viscous dissipation, chemical reaction, radiation and heat generation which are used in the modeled laws. They presented the numerical solution via finite difference technique and established a comparative analysis to judge the scheme efficiency and results validity. They have shown an increase in momentum and thermal profile against electric parameter. Besthapu et al. [8] worked on thermally stratified dissipated stretched nanofluid past over a heating stretching porous sheet numerically. They plotted the solution against different physical parameters and noticed the decline in fluid velocity against magnetic parameter and increase in concentration and thermal fields. Also, they reported the rise in concentration and temperature profiles against mounting values of thermophoresis parameter. Ramzan et al. [9] discussed the optimal solution foe Maxwell nanofluid model with thermal and mass transportation having soret and dufour effects past over a porous heated sheet. They presented the error analysis graphically against different approximations order. They noticed the diminishing impact of porous parameter on velocity. Also, an enhancement in heat and mass transfer coefficients is monitored by them against suction parameter and viscoelastic parameter. Modelling of water based nanoparticles in rotating disc having Darcy Forchhiemer medium with slip effects was analyzed by Hayat et al. [10] analytically. They have mixed different type of nanoparticles in water to investigate thermal performance. They used the relation proposed by Xue for thermos-physical properties. They monitored the enhancement in heat transfer coefficient against Forchhiemer number and retardation in fluid velocity for higher volume fraction. Khanafer and Vafai [11] deliberated the experimental analysis for thermophysical features of nanofluids. They have critically studied different effective viscosity models and thermal expansion coefficient in their reported study. Kempannagari et al. [12] discussed characteristics of heat transfer in micropolar liquid including the effects of thermal conductivity (variable), thermal radiation and Joule heating past a heated curved sirafce. Kumar et al. [13] discussed the aspects of thermal energy in hybrid ferrofluid considering the impacts of thermal radiation and heat generation. Kumar et al. [14] addressed the phenomenal contrast in view of heat transfer and flow behavior over wedge and heated cone. They considered the theory of non-Fourier's under the action of magnetic field via shooting approach. They also investigated that flow phenomena and heat transfer for the case of cone are higher than flow phenomena and heat transfer for the case of wedge. Kumar et al. [15] studied influences of thermal energy along with thermal radiation in the attendance of magnetic field past a heated curved surface via shooting scheme. Kumar et al. [16] captured the behavior of micropolar fluid including the BCs (2^{nd} order and first order slips) whereas they considered variable heat (sink) and Lorentz force. Kumar et al. [17] investigated the flow situation in the attendance of magnetic field. They used slandering heated surface to know the behavior considering effects along with viscous dissipation. Anantha Kumar et al. [18] observed rheology of micropolar fluid along with stagnation point and magnetic field. They used second-order (velocity slip) of considered flow model past a heated vertical surface. They also considered the thermal conductivity (variable), Joule heating and heat source sink and electrical energy. Ashwinkumar [19] visualized the influences of thermal energy and solute particles along with action of magnetic field inserting nanoparticles (alloy/silver-water) past an elongated heated surface. Ashwinkumar and Sulochana et al. [20] simulated consequences buoyancy force and thermal radiation under the action of magnetic field inserting $Al_{50}Cu_{50}$-nanoparticles in the rheology of Casson fluid. Ashwinkumar et al. [21] securitized features of ferrous nanoparticles under the action of magnetic field over melting vertical plate (semi-infinite). Sulochana et al. [22] discussed the aspects of heat transfer phenomena in Maxwell liquid including the nanoparticles over a melting elongated surface. They considered various kinds of influences (heat generation, thermophoresis, Brownian moment and magnetic field) simulated the results via shooting scheme. Mabood et al. [23] discussed an enhancement in thermal energy inserting the

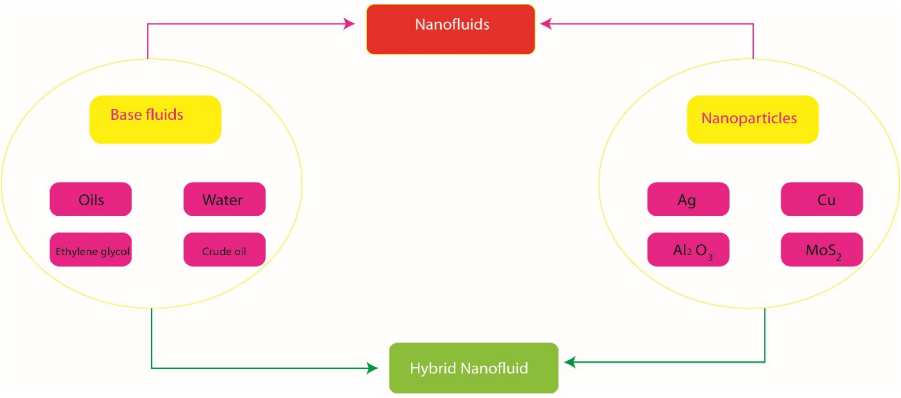

Fig 1. Manufacturing approach of hybrid nanoparticles and nanoparticles.

https://doi.org/10.1371/journal.pone.0256302.g001

hybrid nanoparticles (Fe3O4/graphene–H_20) in the attendance of magnetic field. Mabood et al. [24] simulated the maximum production of heat energy due the role hybrid nanoparticles under the action of thermal radiation and magnetic field past a slandering melting surface. They used shooting scheme to simulate the simulations of considered model. Samrat et al. [25] investigated the rheology of Casson liquid inserting nanoparticles in the presence of thermal rediation past a stretching surface. Sulochana et al. [26] discussed the phenomena of thermal energy in the rheology of ferrofluid involvement of nanoparticles towards the horizontal needle via magnetic field. They studied the role of ferrous nanoparticles in solute particles and thermal energy including magnetic field and thermal radiation subjected to chemical reaction over an elongated plate. Sulochana et al. [27] studied the impact of 2D flow, thermal energy and mass diffusion inserting nanoparticles under action of thermal radiation and chemical reaction over a heated elongated plate via shooting scheme. Some important contributions are reported in [28–36].

Above cited studies ensure that no analysis has been done for hyperbolic tangent model with thermal relaxation time and radiation phenomenon. This contribution fills this gap. This contribution is organized as: section 1 consists of literature survey, modeling of considered flow situation with physical quantities are listed in section 2, solution methodology with advantages is reported in section 3, graphical and tabular results are analyzed in section 4 and section 5 contains the important findings. The sketched scheme of hybrid nanoparticles and nanoparticles are illustrated by Fig 1.

2. Modeling development

The modeling of 2D hyperbolic tangent liquid [1–5] inserting the thermal properties of nano and hybrid nanostructures is addressed past a melting surface. The non-Fourier's law [14, 36] in the presence of heat generation is studied in energy equation. The movement in fluid particles is responsible due to velocity (bx) of surface. The role of magnetic induction is captured and magnetic field is also taken at away from the surface considered by H_0x. The base fluid is considered as a EG (ethylene glycol) along with hyperbolic tangent liquid while nanoparticles (Ag) and hybrid nanoparticles are called MoS_2/Ag. The geometrical phenomenon is demonstrated by Fig 2. The considerations of current model are addressed below:

- Two dimensional flow in the presence of hyperbolic tangent liquid is considered;
- Cattaneo-Christove heat flux is addressed;

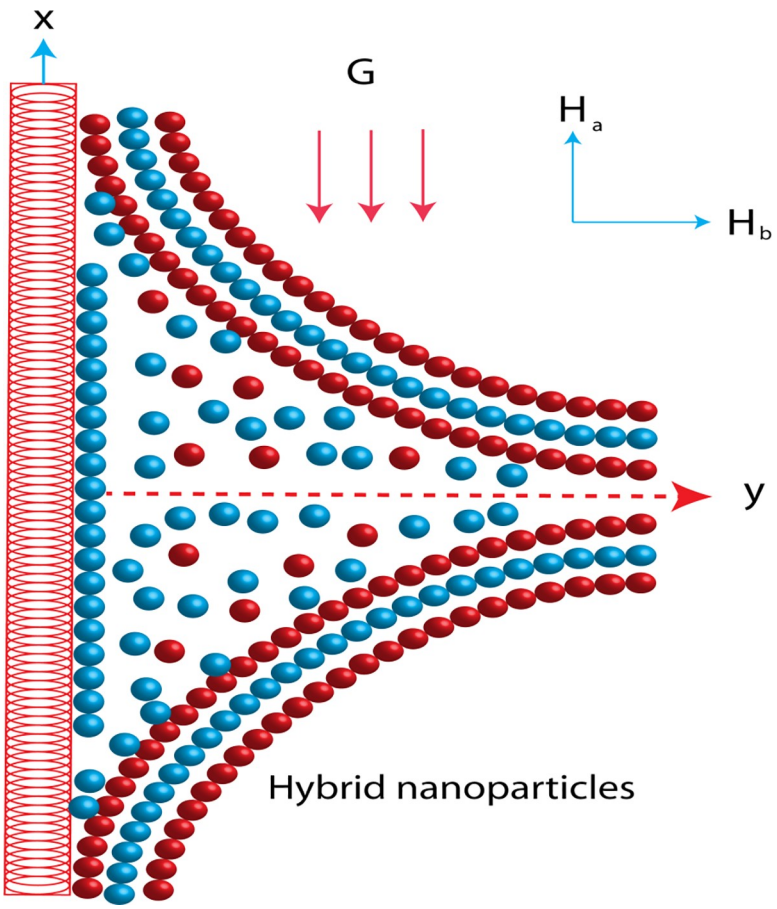

Fig 2. Geometrical view of flow model.

https://doi.org/10.1371/journal.pone.0256302.g002

- The role of heat generation is assumed;
- Steady flow is taken out;
- The behavior of magnetic induction is captured;
- Hybrid nanoparticles and nanoparticles are inserted;
- Thermal properties and correlations of Ag and MoS_2/Ag in ethylene glycol;
- 2^{nd} law analysis associated with mixed convection is observed;
- The vertical melting surface is considered.

The set of PDEs [35] are generated using (BLA) boundary layer approximations which are

$$\frac{\partial \tilde{U}}{\partial x}+\frac{\partial \tilde{V}}{\partial y}=0, \tag{1}$$

$$\frac{\partial H_a}{\partial x}+\frac{\partial H_b}{\partial y}=0, \tag{2}$$

$$\tilde{U}\frac{\partial \tilde{U}}{\partial x}+\tilde{V}\frac{\partial \tilde{U}}{\partial y}-\frac{\tilde{\mu}}{4(\pi)\rho_f}\left(H_a\frac{\partial H_a}{\partial x}+H_b\frac{\partial H_b}{\partial y}\right)=\frac{\mu_f}{A_2A_1}\left[(1-m)\frac{\partial^2\tilde{U}}{\partial y^2}+m\sqrt{2}\Gamma^1\left(\frac{\partial \tilde{U}}{\partial y}\right)\frac{\partial^2\tilde{U}}{\partial y^2}\right] \quad (3)$$

$$+G\frac{(\rho\beta)_f}{\rho_f}A_5(T-T_\infty)-\frac{\tilde{\mu}}{4(\pi)\rho_f}H_e\left(\frac{dH_e}{dx}\right)+U_\infty\frac{dU_\infty}{dx}, \quad (4)$$

$$\tilde{U}\frac{\partial H_a}{\partial x}+\tilde{V}\frac{\partial H_b}{\partial y}=\mu_e\frac{\partial^2 H_a}{\partial y^2}+H_a\frac{\partial \tilde{U}}{\partial x}+H_b\frac{\partial \tilde{U}}{\partial y}, \quad (5)$$

$$\tilde{U}\frac{\partial T}{\partial x}+\tilde{V}\frac{\partial T}{\partial y}+\lambda_A\left(\begin{array}{c}\tilde{U}\frac{\partial \tilde{U}}{\partial x}\frac{\partial T}{\partial x}+\tilde{V}\frac{\partial \tilde{V}}{\partial y}\frac{\partial T}{\partial x}+\tilde{U}\frac{\partial \tilde{V}}{\partial x}\frac{\partial T}{\partial y}+2\tilde{U}\tilde{V}\frac{\partial^2 T}{\partial x\partial y}\\ \tilde{U}^2\frac{\partial^2 T}{\partial x^2}+\tilde{V}^2\frac{\partial^2 T}{\partial y^2}-\frac{Q}{(\rho C_p)_{hnf}}\left(\tilde{U}\frac{\partial T}{\partial x}+\tilde{V}\frac{\partial T}{\partial y}\right)\end{array}\right)=\frac{k_{hnf}}{(\rho C_p)_{hnf}}\frac{\partial^2 T}{\partial^2 y}+Q(T-T_\infty). \quad (6)$$

Where $\tilde{U}, \tilde{V}$ (velocity components), *x*,*y* (space coordinates), *m* (power law index number), $\tilde{H}$ (induced magnetic number), H_a, H_b (components of magnetic induction), $\tilde{\mu}$ (magnetic permeability), μ_e (magnetic diffusivity), *T* (fluid temperature), ρ (fluid density), T_∞ (ambient temperature), *Q* (heat generation), *k* (thermal conductivity), λ_A (relaxation number), *G* (gravitation force), μ_f (fluid dynamic viscosity), Γ^1 (time constant number) and β (thermal expansion) are mentioned above.

No-slip theory provides required boundary conditions (BCs) are

$$\tilde{U}=cx=U_w, \tilde{V}=0, T=T_w, \frac{\partial H_a}{\partial y}=0, H_b=0, y=0,$$
$$\tilde{U}\rightarrow(ax), T=T_\infty, H_a\rightarrow xH_0, y\rightarrow\infty. \quad (7)$$

The variables are used to obtain ODEs and these variables are:

$$\tilde{U}=cxf_\eta, \tilde{V}=-(cv_f)^{\frac{1}{2}}f, \eta=y\left(\frac{c}{v_f}\right)^{\frac{1}{2}},$$
$$H_a=H_0xg_\eta, H_b=-(cv_f)^{\frac{1}{2}}g, \theta(T_w-T_\infty)=T-T_\infty, \quad (8)$$

The system of ODEs along with desired BCs are addressed [35] as

$$\left.\begin{aligned}(1-m)f_{\eta\eta\eta}+mWef_{\eta\eta}f_{\eta\eta\eta}-A_1A_2(f'^2-ff''-A^2)+A_1A_2\beta(g'^2-gg''-1)\\+A_5A_1A_2\lambda_1\theta=0,\\f(0)=0,f_\eta(0)=1,f_\eta(\infty)\to A,\end{aligned}\right\},\tag{9}$$

$$\left.\begin{aligned}g_{\eta\eta\eta}+\frac{1}{\lambda}\left(fg_{\eta\eta}-f_{\eta\eta}g\right)=0,\\g(0)=0,g_{\eta\eta}(0)=1,g_\eta(\infty)\to 1\end{aligned}\right\},\tag{10}$$

$$\left.\begin{aligned}\theta_{\eta\eta}+\frac{k_f(\rho C_p)_{hnf}}{k_{hnf}(\rho C_p)_f}Prf\theta_\eta-\frac{k_f(\rho C_p)_{hnf}}{k_{hnf}(\rho C_p)_f}Pr\Omega_a[ff_\eta\theta_\eta+f^2\theta_{\eta\eta}+H_sf\theta_\eta]\\+\frac{k_f}{k_{hnf}}H_sPr\theta=0,\\\theta(0)=1,\theta(\infty)=0.\end{aligned}\right\}.\tag{11}$$

The correlations of thermo-physical properties in nano and hybrid nanoparticles are mentioned below and their values are listed in Table 1.

$$\left.\begin{aligned}\rho_{nf}=(1-\phi)\rho_f+\phi\rho_s,\rho_{hnf}=[(1-\phi_2)\{(1-\phi_1)\rho_f+\phi_1\rho_{s1}\}]+\phi_2\rho_{s2},\\(\rho C_p)_{nf}=(1-\phi)(\rho C_p)_f+\phi(\rho C_p)_s,(\rho C_p)_{hnf}=\left[(1-\phi_2)\left\{\begin{matrix}(1-\phi_1)(\rho C_p)_f\\+\phi_1(\rho C_p)_{s_1}\end{matrix}\right\}\right]\\+\phi_1(\rho C_p)_{s_2},\end{aligned}\right\}\tag{12}$$

$$\left.\begin{aligned}\mu_{nf}=\frac{\mu_f}{(1-\phi)^{2.5}},\mu_{nf}=\frac{\mu_f}{(1-\phi_2)^{2.5}(1-\phi_1)^{2.5}},\frac{k_{nf}}{k_f}=\left\{\frac{k_s+(n+1)k_f-(n-1)\phi(k_f-k_s)}{k_s+(n-1)k_f+\phi(k_f-k_s)}\right\},\\\frac{k_{hnf}}{k_{bf}}=\left\{\frac{k_{s_2}+(n-1)k_{bf}-(n-1)\phi_2(k_{bf}-k_{s_2})}{k_{s_2}+(n-1)k_{bf}-\phi_2(k_{bf}-k_{s_2})}\right\},\frac{\sigma_{hnf}}{\sigma_f}=\left(1+\frac{3(\sigma-1)\phi}{(\sigma+2)-(\sigma-1)\phi}\right),\\\frac{\sigma_{hnf}}{\sigma_f}=\left(\frac{\sigma_{s_2}+2\sigma_f-2\phi_2(\sigma_{bf}-\sigma_{s_2})}{\sigma_{s_2}+2\sigma_f+\phi_2(\sigma_{bf}-\sigma_{s_2})}\right),\frac{\sigma_{bf}}{\sigma_f}=\left(\frac{\sigma_{s_1}+2\sigma_f-2\phi_1(\sigma_f-\sigma_{s_1})}{\sigma_{s_1}+2\sigma_f+\phi_1(\sigma_f-\sigma_{s_1})}\right)\end{aligned}\right\}\tag{13}$$

Table 1. Properties related to thermal of nanoparticles and hybrid nanoparticles in EG.

MoS_2	Ag	$C_2H_6O_2$
$\rho_{MoS_2}(=5060)$	$\rho_{Ag}(=10490)$	$\rho_{C_2H_6O_2}(=1113.5)$
$(C_p)_{MoS_2}(=397.21)$	$(C_p)_{Ag}(=235)$	$(C_p)_{C_2H_6O_2}(=2430)$
$k_{MoS_2}(=904.4)$	$k_{Ag}(429)$	$k_{C_2H_6O_2}(=0.253)$
$\beta_{MoS_2}(=2.8424\times10^{-5})$	$\beta_{Ag}(=1.89\times10^{-5})$	$\beta_{C_2H_6O_2}(=5.8\times10^{-4})$
$\sigma_{MoS_2}(=2.09\times10^{-5})$	$\sigma_{Ag}(=6.30\times10^{7})$	$\sigma_{C_2H_6O_2}(=4.3\times10^{-5})$

https://doi.org/10.1371/journal.pone.0256302.t001

$$\left.\begin{aligned} A_1 = (1-\phi_2)^{\frac{5}{2}}(1-\phi_1)^{\frac{5}{2}}, A_2 = (1-\phi_2)\left[1-\phi_1+\phi_1\frac{\rho_{s_1}}{\rho_f}\right]+\phi_2\frac{\rho_{s_2}}{\rho_f}, \\ A_3 = \left[1-\phi_1+\phi_1\frac{(\rho c_p)_{s_1}}{(\rho c_p)_f}\right]+\phi_2\frac{(\rho c_p)_{s_2}}{(\rho c_p)_f}, \\ A_5 = \frac{\phi_2\frac{(\rho\beta)_{s_2}}{(\rho\beta)_f}+\left[(1-\phi_1-\phi_2)+\phi_2\frac{(\rho\beta)_{s_2}}{(\rho\beta)_f}\right]}{(1-\phi_1)\left[(1-\phi_1)+\phi_2\frac{\rho s_1}{\rho_f}\right]+\phi_2\frac{\rho s_2}{\rho_f}}. \end{aligned}\right\} \quad (14)$$

Here ϕ_2, ϕ_1, ϕ (volume fractions), *hnf* (hybrid nanoparticles) and *nf* (nanoparticles) are considered in Eqs (9–14). Further, *Pr* (Prandtl number), λ (magnetic Prandtl number in term of reciprocal), β (magnetic number), *A* (stretching ratio number), H_s (heat generation number), λ_1 (mixed convection number), Ω_a (relaxation number) and *We* (Weissenberg number) are addressed as:

$$Pr = (\mu C_p)_f (k_f)^{-1}, \lambda = \frac{\mu_e}{\nu_f}, \beta = \frac{\tilde{\mu}H_0^2}{c^2\rho_f 4\pi}, A = \frac{a}{c},$$

$$H_s = \frac{Q}{c(\rho C_p)_f}, \lambda_1 = \frac{g\beta(T_w - T_\infty)}{xc^2}, \Omega_a = b\lambda_A, We = \left(\frac{c^3\Gamma x^2}{\nu_f}\right)^{1/2}.$$

The divergent velocity at melting surface is derived as

$$C_f = \frac{\tau_{xy|y=0}}{\rho_f(bx)^2}, \sqrt{R_e}C_f = \frac{-1}{(1-\phi_2)^{5/2}(1-\phi_1)^{5/2}}\left[(1-m)f_{\eta\eta}(0) + \frac{m}{2}We(f_{\eta\eta}(0))^2\right].$$

The temperature gradient of current phenomenon is

$$Nu = \frac{-xk_{hnf}\frac{\partial T}{\partial y}|_{y=0}}{(T_w - T_\infty)k_f}, (R_e)^{-1/2}Nu = -\frac{k_{hnf}}{k_f}\theta_\eta(0),$$

where (Reynolds number) $Re\left(=\frac{U_w x}{\nu_f}\right)$.

3. Solution scheme and convergence analysis

The non-linear ODEs are numerically simulated using numerical scheme called finite element approach [33, 34]. Such numerical approach has ability to compute numerical solution of current complex problem. The main steps related this scheme is discussed here:

- The residuals (weighted integral) are made whereas the residuals are made using the integrating approach in set of non-linear ODEs (ordinary differential equations);
- In next step, computational domain is achieved through problem domain considering [0, ∞). It is demonstrated that numerical computations reveal that asymptotic BCs are agreed at $\eta_\infty = 7$. Hence, [0, 7] is considered as computation domain;

Table 2. Convergence analysis of velocities and thermal energy considering 300 elements.

Number of elements	$f'\left(\frac{\eta_\infty}{2}\right)$	$g'\left(\frac{\eta_\infty}{2}\right)$	$\theta\left(\frac{\eta_\infty}{2}\right)$
30	0.4853074	0.5326158	0.5946054
60	0.4568591	0.5163933	0.5772373
90	0.4476232	0.5110348	0.5716849
120	0.4429796	0.5082616	0.5687690
150	0.4402813	0.5066645	0.5668638
180	0.4384072	0.5055560	0.5660132
210	0.4371181	0.5047064	0.5644715
240	0.4361482	0.5041676	0.5641853
270	0.4353591	0.5036810	0.5637239
300	0.4347759	0.5033553	0.5634322

https://doi.org/10.1371/journal.pone.0256302.t002

- The stiffness matrix is computed using GFEA (Galerikin finite element approximation) in weak form of residuals (weighted integrals). The stiffness elements along with 300 elements in integral residuals are made. Finally, assembly scheme is captured;
- A Picard linearization scheme is utilized to make linearization in algebraic equations. The tolerance is captured as 10^{-8} for solving equations;
- The convergence approach is addressed considering 300 elements. Hence, current problem is converged at mid of each 300 elements. This convergence study is simulated in Table 2. Each outcome is simulated at the mid of each element. The validation of numerical results related to gradient temperature is simulated by Table 3.

4. Results and discussion

The code related to finite element approach called Galerikin finite element scheme is developed in Maple 18. This numerical approach has ability to simulate the complex flow problems. The current problem is addressed physical happening in view of PDEs including characterizations magnetic induction and non-Fourier's theory. In this section, prime graphical outcomes of motion and thermal energy in fluid particles in the presence of heat enhancement role of nano and hybrid nanoparticles versus variation parameters are simulated. The prime discussion is addressed below:

4.1 Graphical outcomes of flow situation

The measurement of flow situation is addressed versus the variation in We (Weissenberg number), H_s (heat generation number), λ_1 (mixed convection number) and m (power law index number) inserting the nanoparticles and hybrid-nanostructures is captured. It is investigated

Table 3. Comparison of simulations in view of Nusselt number when ϕ_1 =0, ϕ_2 = 0, A = 3.0, β = 1.

Pr	Iqbal et al. [35]	Present results
0.07	0.33814	0.3387103
0.5	0.82748	0.8273089
2.0	1.52147	1.5239940
6.8	2.59780	2.5971029
10.0	3.07902	3.0698597

https://doi.org/10.1371/journal.pone.0256302.t003

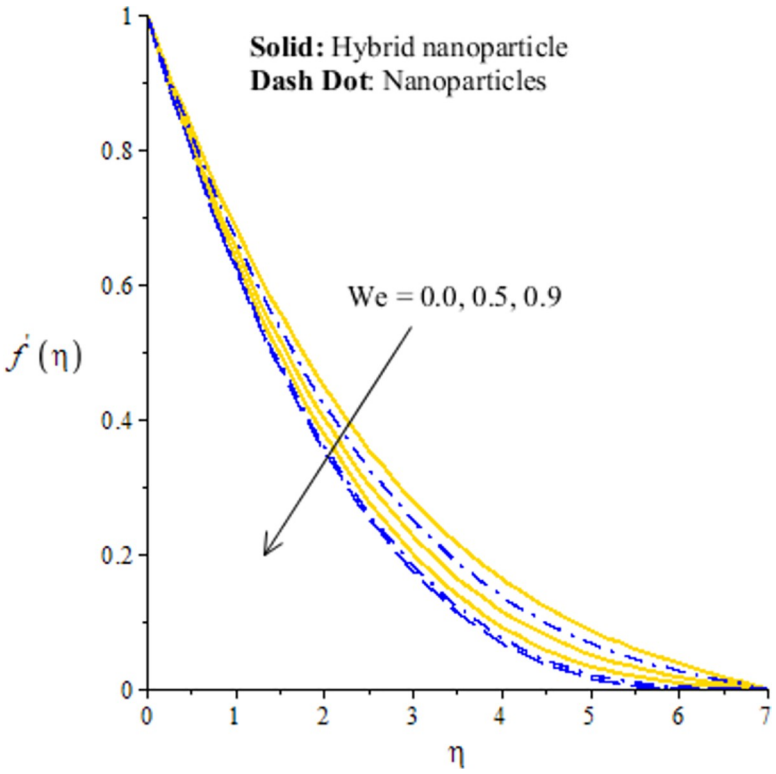

Fig 3. Distribution of velocity versus *we*.

https://doi.org/10.1371/journal.pone.0256302.g003

that solid curves reveal that role of nanoparticles while dash dot lines are generated the influence of hybrid nanoparticles considering by Figs 3–10. Further, *Ag* is called nanoparticles and composite of *Ag* and MoS_2 is known as hybrid nanoparticles. Fig 3 illustrates graphical variation in flow of nano and hybrid nanoparticles taking higher values of Weissenberg number. It is noticed that the concept of Weissenberg number is modeled due to the appearance of hyperbolic tangent tensor in momentum equation. Therefore, role of *We* is observed on the flow. In this figure, (*We*) generates the retardation force in motion of particles and this retardation force makes the reduction in flow speed of fluid particles. Physically, *We* is the ratio of viscous forces and elastic forces and viscous forces are increased during the flow of nanoparticles and hybrid nanoparticles versus the higher values of (*We*). So, higher viscous forces create the resistance force during flow of fluid particles when (*We*) is enhanced. Hybrid nanoparticles are more efficient in view of flow speed as compared nanoparticles. The distribution of flow speed is measured against the variation of power law index number (see Fig 4). The numerical values of *m* decides flow behavior whereas *m* is occurred due to tensor of hyperbolic tangent liquid. For $m = 0$, the fluid becomes Newtonian liquid and fluid becomes shear thickening using $m<0$. The flow becomes thick using large values of *m*. Therefore, *m* is not favorable as physical parameter to obtain the maximum flow speed. Hence, decreasing trend is measured against enlargement in *m*. From Fig 4, study of hybrid nanoparticles is favorable rather than nanoparticles in base fluid called ethylene glycol. Figs 5 and 7 demonstrate the flow situation versus the variation of λ_1. The increment in flow behavior is found against the large value of λ_1. This parameter generates maximum magnitude in flow and maximum flow speed is happened due to higher temperature gradient. The maximum convection and bouncy force are generated due to large temperature gradient in primary flow as well in secondary flow.

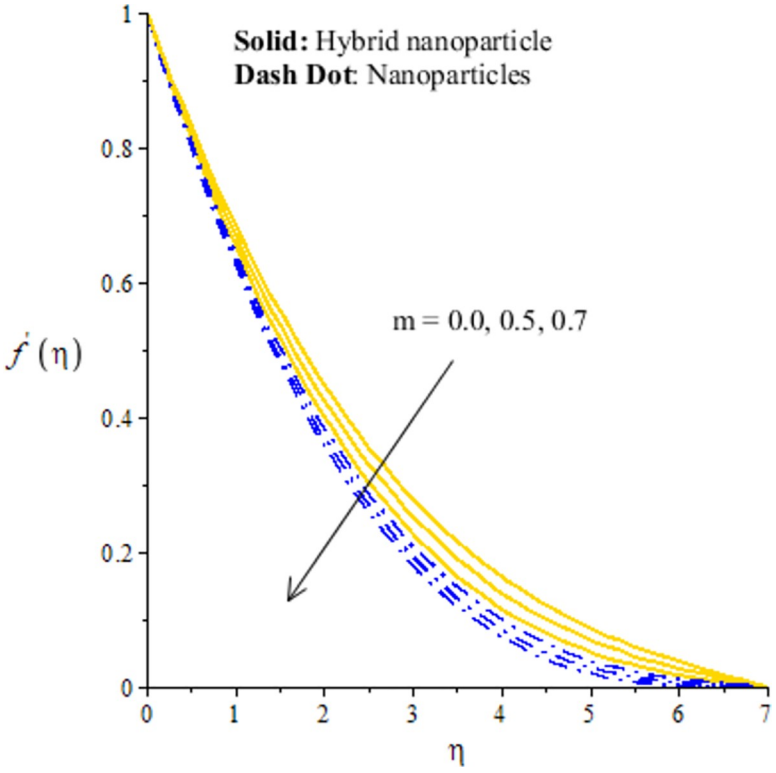

Fig 4. Distribution of velocity versus *m*.

https://doi.org/10.1371/journal.pone.0256302.g004

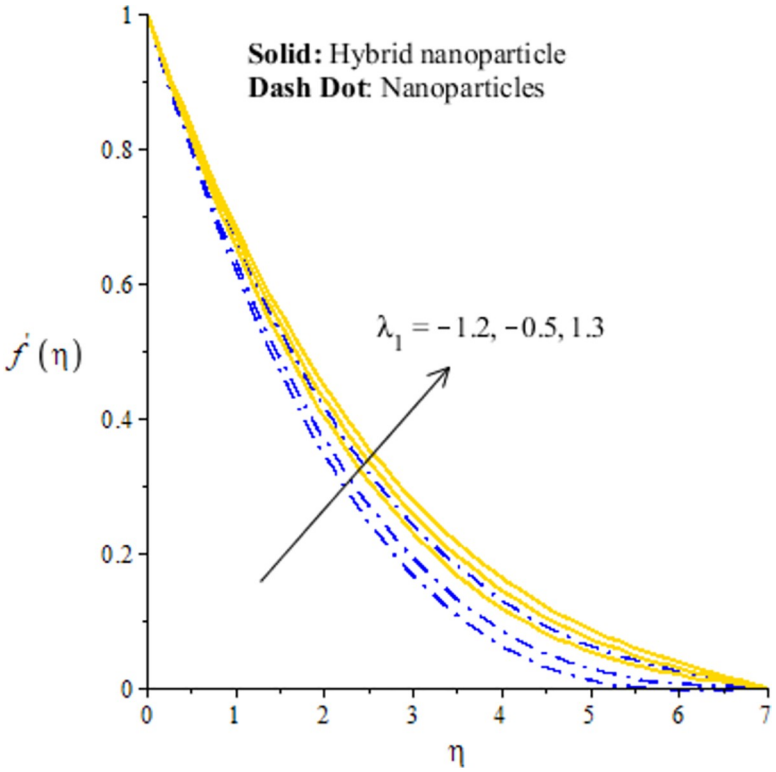

Fig 5. Distribution of velocity versus λ_1.

https://doi.org/10.1371/journal.pone.0256302.g005

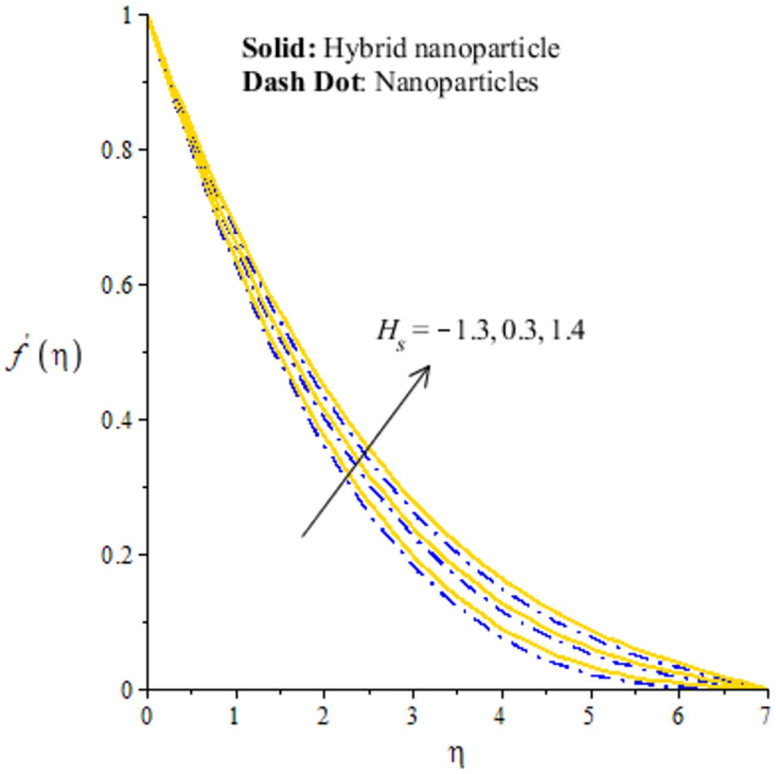

Fig 6. Distribution of velocity versus H_s.

https://doi.org/10.1371/journal.pone.0256302.g006

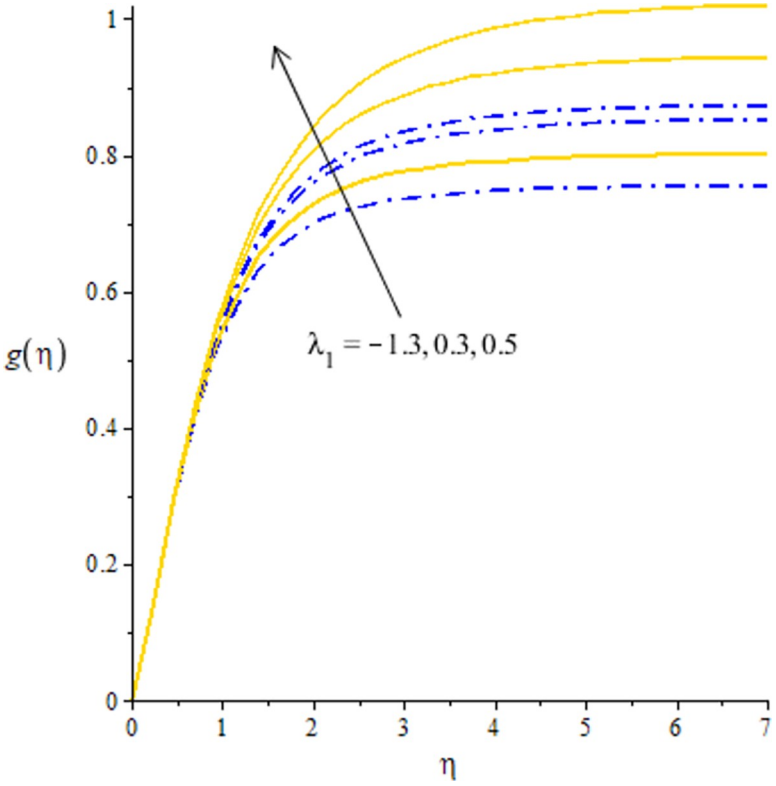

Fig 7. Distribution of velocity versus λ_1.

https://doi.org/10.1371/journal.pone.0256302.g007

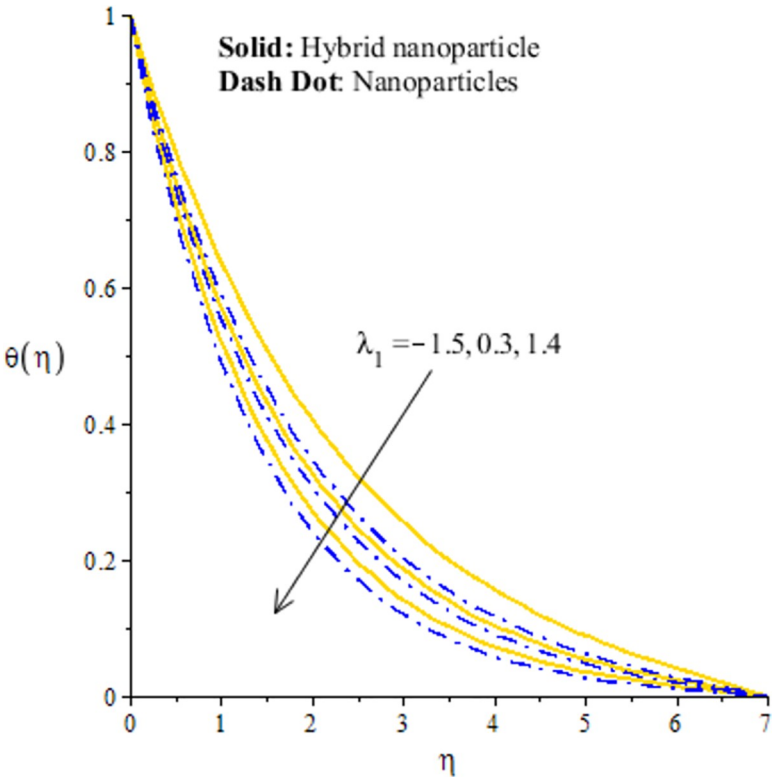

Fig 8. Distribution of temperature versus λ_1.

https://doi.org/10.1371/journal.pone.0256302.g008

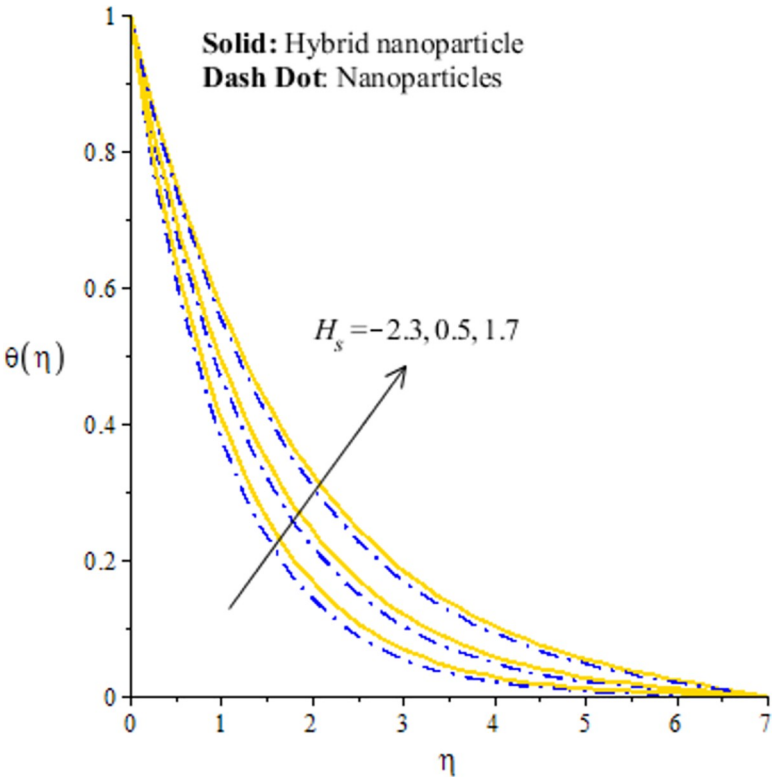

Fig 9. Distribution of temperature versus H_s.

https://doi.org/10.1371/journal.pone.0256302.g009

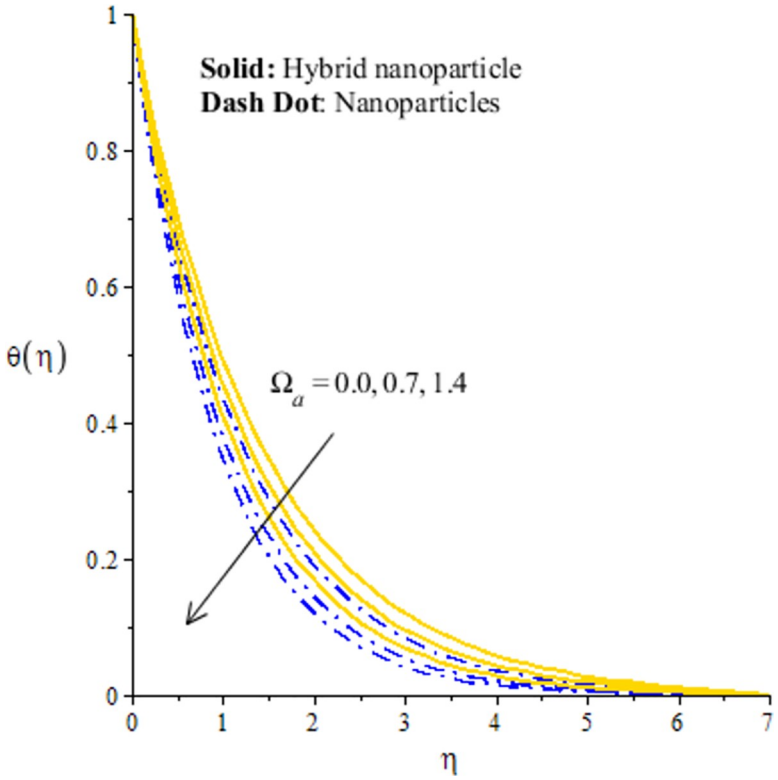

Fig 10. Distribution of temperature versus Ω_a.

https://doi.org/10.1371/journal.pone.0256302.g010

Meanwhile, bouncy force has a direct relation versus the pressure gradient which generates the maximum magnitude in MBL (momentum boundary layer thickness). The values of $\lambda_1>0$ and $\lambda_1<0$ are associated along with the role of cooling and heating processes in fluid particles. In graphical view, cooling process is considered for decrement in flow and heating process is assumed for increasing flow. Moreover, nanoparticles are not enough significant to obtain maximum flow as compared maximum flow for hybrid nanoparticles. Hence, the change in λ_1 becomes favorable physical parameter against temperature gradient and bouncy force. This happening derives the fluid significant over heated surface. Here, dual role of λ_1 is notices against flow. The thickness related (BL) is increased using the higher values of λ_1. The variation in H_s against the primary velocity is conducted by Fig 6. The flow is enhanced using enlargement in H_s. The internal heat in fluid particles are increased due to H_s and internal heat has direct relation versus kinetic energy. Hence, direct relation is simulated versus H_s. Therefore, MBL become significant. The large values of H_s produces more heat energy into fluid particles. Therefore, heat energy of hybrid nanoparticles and nanoparticles is increased. It is noticed that property related to generative of heat energy is not suitable when hybrid nanoparticles are considered as a coolant.

4.2 Graphical outcomes of thermal energy

The measurement of temperature is essential part in this research article. In fact, comparative simulations are captured inserting nano and hybrid nano-structures in base fluid versus H_s, Ω_a and λ_1. In Figs 8–10, it is essential to mention that hybrid nanoparticles are more efficient to obtain maximum enhancement in thermal conductivity rather than the role of nanoparticles. Therefore, hybrid nanoparticles are efficient strong to achieve maximum production of heat

energy and cooling process. Fig 8 conducts the distribution of thermal energy against λ_1. The reduction in the production of heat energy is achieved versus the higher λ_1. In physical point of view, temperature gradient enhances due to large values of λ_1 and more acceleration is produced in velocity. Physically, flow of fluid particles accelerates and temperature gradient increases due to higher values of λ_1. These dual influences enhance the flow and thermal energy transfer. Further, These dual influences decrees internal energy of particles. Hence, these happenings create decline in temperature profile. The solid curves are higher than curved related to das dot lines. The graphical study with respect to H_s is addressed by Fig 9. The fluid particles are heated due internal energy source. So, more heat is generated in fluid particles using H_s. The large values of H_s produces more heat energy into fluid particles. Therefore, heat energy of hybrid nanoparticles and nanoparticles is increased. It is noticed that external heat source is considered at surface of sheet generate more heat into fluid particles. Hence, fluid particles are heated due to enhancement of heat generation number. Therefore, increasing function is conducted of heat energy. Moreover, maximum amount of heat energy is captured inserting hybrid nanoparticles rather than inserting the nanoparticles. Fig 10 addresses decreasing character of heat energy against the change in Ω_a. It is noticed that Ω_a is constructed due to non-Fourier's concept using in energy equation. The role of Ω_a is not favorable to attain the maximum production in heat energy. The current study is transformed into the case of Fourier's law for $\Omega_a = 0$. Finally, the case regarding Fourier's law is more significant to attain maximum heat energy as compared the non-Fourier's theory. Here, Ω_a denotes the phenomena of thermal relaxation. The higher values of thermal relaxation time enhance the performance of fluid related to restore the equilibrium condition. This effect brings minimizing change into the thermal state of fluid particles. Therefore, it has direct effect on TBL (thermal boundary layer thickness).

4.3 Outcomes related to gradient temperature and divergent flow

The divergent flow and gradient temperature are noticed versus We, λ_1, H_s and Ω_a simulating in Table 4. The reduction in gradient called skin friction coefficient versus variation in We and λ_1 but increasing values of divergent flow is simulated against We. Physically, flow of fluid particles accelerates and temperature gradient increases due to higher values of λ_1. These dual influences enhance the flow and thermal energy transfer. Further, These dual influences decrees internal energy of particles. In comparative view, hybrid nanoparticles make the more

Table 4. Comparative simulations of gradient temperature and skin friction coefficient considering nanoparticles and hybrid nanoparticles versus the change in We, λ_1, H_s and Ω_a.

		Nanoparticles		Hybrid nanoparticles	
		$-(R_e)^{1/2}C_f$	$-(R_e)^{-1/2}Nu$	$-(R_e)^{1/2}C_f$	$-(R_e)^{-1/2}Nu$
	0.0	0.40101802	0.31201902	1.01219001	2.13201732
We	0.2	0.36352971	0.44888821	1.20065603	2.55502285
	0.7	0.22859163	0.41301203	1.335083774	2.31001730
	0.7	0.417202388	0.34110303	1.413212063	2.23210163
λ_1	-1.3	0.3082075083	0.44888821	1.510071963	3.55502285
	0.3	0.2082084230	0.53410120	1.310072391	3.73210132
	1.2	0.1082089891	0.61004305	1.210072658	3.91213031
H_s	-1.2	0.5082209234	0.77329020	2.710090674	3.27237837
	0.5	0.2101789003	0.401603593	2.231073203	3.008146408
	0.0	0.0083779234	1.3123635	0.010284611	3.3180474
Ω_a	0.5	0.0083779234	1.5012340	0.010284611	3.4231303
	1.5	0.0083779234	1.7092120	0.010284611	3.7121313

https://doi.org/10.1371/journal.pone.0256302.t004

enhancements in divergent flow as compared nanoparticles. Hence, nanoparticles are more essential rather than study of nanoparticles in view of divergent velocity. The gradient temperature is enhanced versus heat generation number due to gravitational force. But inverse trend is simulated in temperature gradient due to using the large values of Ω_a. Meanwhile, it is observed that study of hybrid nanoparticles make the more impact to attain maximum temperature gradient called Nusselt number rather than the study of nanoparticles.

5. Conclusion and prime findings

The features of magnetic induction in tangent hyperbolic liquid suspending with nanoparticles and hybrid nano-structures is addressed. The role of non-Fourier's theory along with heat generation is considered. This complex model is simulated with strong technique called finite element approach (FEM). The prime outcomes related to current model is captured below:

- The hybrid nanoparticles are more efficient to conduct maximum production of heat energy as compared the production of heat energy of nanoparticles. Hence, hybrid nanoparticles (MoS_2/Ag) are observed more significant to conduct more heat energy rather than nanoparticles (Ag);
- The flow is significantly enhanced for the case of hybrid nanomaterials as compared for the case nanomaterials. The flow of hybrid nanoparticles is higher than flow of nanoparticles considering various physical parameters;
- The convergence of current model is analyzed up to 300 elements. The implementation of FEM is considered very useful for discretization of derivatives and this approach handles various types BCs (boundary conditions);
- The power law and Weissenberg numbers indicate the reduction in growth of velocity but flow is enhanced versus the large values of heat generation and mixed convection number. The thickness of boundary layers is declined considering higher values of Weissenberg number while thickness of boundary layers in inclined versus the change in power law number;
- The maximum amount of heat energy is simulated using large value heat generation number but less production of heat energy is attained against the variation of time relaxation and mixed convection numbers. Further, thickness related to thermal layers becomes higher versus the values of heat generation number. The variation of time relaxation and mixed convection numbers make the reduction in thermal boundary layer thickness.
- The temperature gradient is enhanced versus enlargement in time relaxation and mixed convection numbers while decimation in temperature gradient is captured using higher values of heat generation and Weissenberg numbers. Moreover, hybrid nanoparticles are also considered useful to maximized production of temperature gradient rather than the production of temperature gradient for the case of nanoparticles;
- The skin friction is reduced versus enhancement in heat generation mixed convection numbers but reverse role is addressed versus the higher values of Weissenberg and mixed convection numbers. The surface force becomes higher for hybrid nanoparticles than surface force for the case of nanoparticles.

Author Contributions

Conceptualization: Muhammad Sohail, Hussam Alrabaiah.

Data curation: Muhammad Sohail, Hussam Alrabaiah, Phatiphat Thounthong.

Formal analysis: Umar Nazir, Muhammad Sohail, Hussam Alrabaiah, Mahmoud M. Selim.

Funding acquisition: Mahmoud M. Selim, Phatiphat Thounthong, Choonkil Park.

Investigation: Umar Nazir, Hussam Alrabaiah.

Methodology: Muhammad Sohail.

Resources: Mahmoud M. Selim.

Software: Muhammad Sohail, Phatiphat Thounthong.

Supervision: Phatiphat Thounthong.

Validation: Umar Nazir.

Visualization: Umar Nazir, Choonkil Park.

Writing – original draft: Umar Nazir, Phatiphat Thounthong.

Writing – review & editing: Umar Nazir, Phatiphat Thounthong.

References

1. Naseer M., Malik M.Y., Nadeem S. and Rehman A., 2014. The boundary layer flow of hyperbolic tangent fluid over a vertical exponentially stretching cylinder. Alexandria engineering journal, 53 (3), pp.747–750.
2. Khan M., Rasheed A., Salahuddin T. and Ali S., 2021. Chemically reactive flow of hyperbolic tangent fluid flow having thermal radiation and double stratification embedded in porous medium. Ain Shams Engineering Journal.
3. Nawaz M., Nazir U., Saleem S. and Alharbi S.O., 2020. An enhancement of thermal performance of ethylene glycol by nano and hybrid nanoparticles. Physica A: Statistical Mechanics and its Applications, 551, p.124527.
4. Ali A., Hussain R. and Maroof M., 2019. Inclined hydromagnetic impact on tangent hyperbolic fluid flow over a vertical stretched sheet. AIP Advances, 9(12), p.125022.
5. Patil M. and Raju C.S.K., 2019. Convective conditions and dissipation on Tangent Hyperbolic fluid over a chemically heating exponentially porous sheet. Nonlinear Engineering, 8(1), pp.407–418.
6. Aman S., Khan I., Ismail Z., Salleh M.Z., Alshomrani A.S. and Alghamdi M.S., 2017. Magnetic field effect on Poiseuille flow and heat transfer of carbon nanotubes along a vertical channel filled with Casson fluid. AIP Advances, 7(1), p.015036.
7. Daniel Y.S., Aziz Z.A., Ismail Z. and Salah F., 2017. Double stratification effects on unsteady electrical MHD mixed convection flow of nanofluid with viscous dissipation and Joule heating. Journal of applied research and technology, 15(5), pp.464–476.
8. Besthapu P., Haq R.U., Bandari S. and Al-Mdallal Q.M., 2017. Mixed convection flow of thermally stratified MHD nanofluid over an exponentially stretching surface with viscous dissipation effect. Journal of the Taiwan Institute of Chemical Engineers, 71, pp.307–314.
9. Ramzan M., Bilal M., Chung J.D. and Farooq U., 2016. Mixed convective flow of Maxwell nanofluid past a porous vertical stretched surface–An optimal solution. Results in Physics, 6, pp.1072–1079.
10. Hayat T., Nasir T., Khan M.I. and Alsaedi A., 2018. Non-Darcy flow of water-based single (SWCNTs) and multiple (MWCNTs) walls carbon nanotubes with multiple slip conditions due to rotating disk. Results in Physics, 9, pp.390–399.
11. Khanafer K. and Vafai K., 2017. A critical synthesis of thermophysical characteristics of nanofluids. Nanotechnology and Energy, pp.279–332.
12. Kempannagari A.K., Buruju R.R., Naramgari S. and Vangala S., 2020. Effect of Joule heating on MHD non-Newtonian fluid flow past an exponentially stretching curved surface. Heat Transfer, 49 (6), pp.3575–3592.
13. Kumar K.A., Sandeep N., Sugunamma V. and Animasaun I.L., 2020. Effect of irregular heat source/sink on the radiative thin film flow of MHD hybrid ferrofluid. Journal of Thermal Analysis and Calorimetry, 139(3), pp.2145–2153.

14. Kumar K.A., Reddy J.R., Sugunamma V. and Sandeep N., 2018. Magnetohydrodynamic Cattaneo-Christov flow past a cone and a wedge with variable heat source/sink. Alexandria engineering journal, 57(1), pp.435–443.

15. Kumar K.A., Sugunamma V. and Sandeep N., 2020. Effect of thermal radiation on MHD Casson fluid flow over an exponentially stretching curved sheet. Journal of Thermal Analysis and Calorimetry, 140 (5), pp.2377–2385.

16. Kumar K.A., Sugunamma V., Sandeep N. and Mustafa M.T., 2019. Simultaneous solutions for first order and second order slips on micropolar fluid flow across a convective surface in the presence of Lorentz force and variable heat source/sink. Scientific reports, 9(1), pp.1–14. https://doi.org/10.1038/s41598-018-37186-2 PMID: 30626917

17. Kumar K.A., Sugunamma V. and Sandeep N., 2020. Influence of viscous dissipation on MHD flow of micropolar fluid over a slendering stretching surface with modified heat flux model. Journal of Thermal Analysis and Calorimetry, 139(6), pp.3661–3674.

18. Anantha Kumar K., Sugunamma V. and Sandeep N., 2019. Physical aspects on unsteady MHD-free convective stagnation point flow of micropolar fluid over a stretching surface. Heat Transfer—Asian Research, 48(8), pp.3968–3985.

19. Ashwinkumar G.P., 2021. Heat and mass transfer analysis in unsteady MHD flow of aluminum alloy/silver-water nanoliquid due to an elongated surface. Heat Transfer, 50(2), pp.1679–1696.

20. Ashwinkumar G.P. and Sulochana C., 2018. Effect of radiation absorption and buoyancy force on the MHD mixed convection flow of Casson nanofluid embedded with $Al_{50}Cu_{50}$ alloy nanoparticles. Multidiscipline Modeling in Materials and Structures.

21. Ashwinkumar G.P., Sulochana C. and Samrat S.P., 2018. Effect of the aligned magnetic field on the boundary layer analysis of magnetic-nanofluid over a semi-infinite vertical plate with ferrous nanoparticles. Multidiscipline Modeling in Materials and Structures.

22. Sulochana C., Ashwinkumar G.P. and Sandeep N., 2017. Effect of thermophoresis and Brownian moment on 2D MHD nanofluid flow over an elongated sheet. In Defect and Diffusion Forum (Vol. 377, pp. 111–126). Trans Tech Publications Ltd.

23. Mabood F., Ashwinkumar G.P. and Sandeep N., 2020. Effect of nonlinear radiation on 3D unsteady MHD stagnancy flow of Fe3O4/graphene–water hybrid nanofluid. International Journal of Ambient Energy, pp.1–11.

24. Mabood F., Ashwinkumar G.P. and Sandeep N., 2020. Simultaneous results for unsteady flow of MHD hybrid nanoliquid above a flat/slendering surface. Journal of Thermal Analysis and Calorimetry, pp.1–13.

25. Samrat S.P., Sulochana C. and Ashwinkumar G.P., 2019. Impact of thermal radiation on an unsteady Casson nanofluid flow over a stretching surface. International Journal of Applied and Computational Mathematics, 5(2), pp.1–20.

26. Sulochana C., Ashwinkumar G.P. and Sandeep N., 2018. Boundary layer analysis of persistent moving horizontal needle in magnetohydrodynamic ferrofluid: A numerical study. Alexandria engineering journal, 57(4), pp.2559–2566.

27. Sulochana C., Ashwinkumar G.P. and SP Samrat S.P., 2018. Impact of thermal radiation and chemical reaction on unsteady 2D flow of magnetic-nanofluids over an elongated plate embedded with ferrous nanoparticles. Frontiers in Heat and Mass Transfer (FHMT), 10.

28. Abdelsalam S.I. and Sohail M., 2020. Numerical approach of variable thermophysical features of dissipated viscous nanofluid comprising gyrotactic micro-organisms. Pramana: Journal of Physics, 94(1).

29. Sohail M., Nazir U., Chu Y.M., Al-Kouz W. and Thounthong P., 2021. Bioconvection phenomenon for the boundary layer flow of magnetohydrodynamic Carreau liquid over a heated disk. Scientia Iranica, 28(3), pp.1896–1907.

30. Sohail M. and Naz R., 2020. Modified heat and mass transmission models in the magnetohydrodynamic flow of Sutterby nanofluid in stretching cylinder. Physica A: Statistical Mechanics and its Applications, p.124088.

31. Qayyum M., Khan O., Abdeljawad T., Imran N., Sohail M. and Al-Kouz W., 2020. On Behavioral Response of 3D Squeezing Flow of Nanofluids in a Rotating Channel. Complexity, 2020.

32. Sohail M., Chu Y.M., El-zahar E.R., Nazir U. and Naseem T., 2021. Contribution of joule heating and viscous dissipation on three dimensional flow of Casson model comprising temperature dependent conductance utilizing shooting method. Physica Scripta.

33. Wong H. F., Sohail M., Siri Z. and N. F., "Numerical solutions for heat transfer of an unsteady cavity with viscous heating," Computers, Materials & Continua, vol. 68, no.1, pp. 319–336, 2021.

34. Nazir U., Nawaz M. and Alharbi S.O., 2020. Thermal performance of magnetohydrodynamic complex fluid using nano and hybrid nanoparticles. Physica A: Statistical Mechanics and its Applications, 553, p.124345. https://doi.org/10.1016/j.physa.2020.124345

35. Iqbal Z., Azhar E. and Maraj E.N., 2017. Utilization of the computational technique to improve the thermophysical performance in the transportation of an electrically conducting Al_2O_3-Ag/H_2O hybrid nanofluid. The European Physical Journal Plus, 132(12), pp.1–13.

36. Kumar K.A., Sugunamma V. and Sandeep N., 2019. A non-Fourier heat flux model for magnetohydrodynamic micropolar liquid flow across a coagulated sheet. Heat Transfer—Asian Research, 48(7), pp.2819–2843. https://doi.org/10.1002/htj.21518